Supporting Information for

Mussel-inspired polymeric coatings with the antifouling efficacy controlled by topologies

Chenxi Xiong, [‡a] Wenjuan Xiong, [‡a] Youbing Mu,[*a] Danfeng Pei [*b] and Xiaobo Wan[*a]

[a.] Key Laboratory of Optoelectronic Chemical Materials and Devices, Ministry of Education, School of Optoelectronic Materials & Technology, Jianghan University, Wuhan 430056, P. R. China. E-mail: muyb@jhun.edu.cn, wanxb@jhun.edu.cn

[b.] Qingdao Institute of Bioenergy and Bioprocess Technology, Chinese Academy of Sciences, Qingdao 210062, P. R. China. E-mail: peidf@qibebt.ac.cn

‡ These authors contributed equally to this work.

1. Synthesis of chain transfer agent

Four kinds of chain transfer agent named EBP-CTA, EG-CTA, TMP-CTA and PE-CTA were synthesized as shown in Scheme S1.

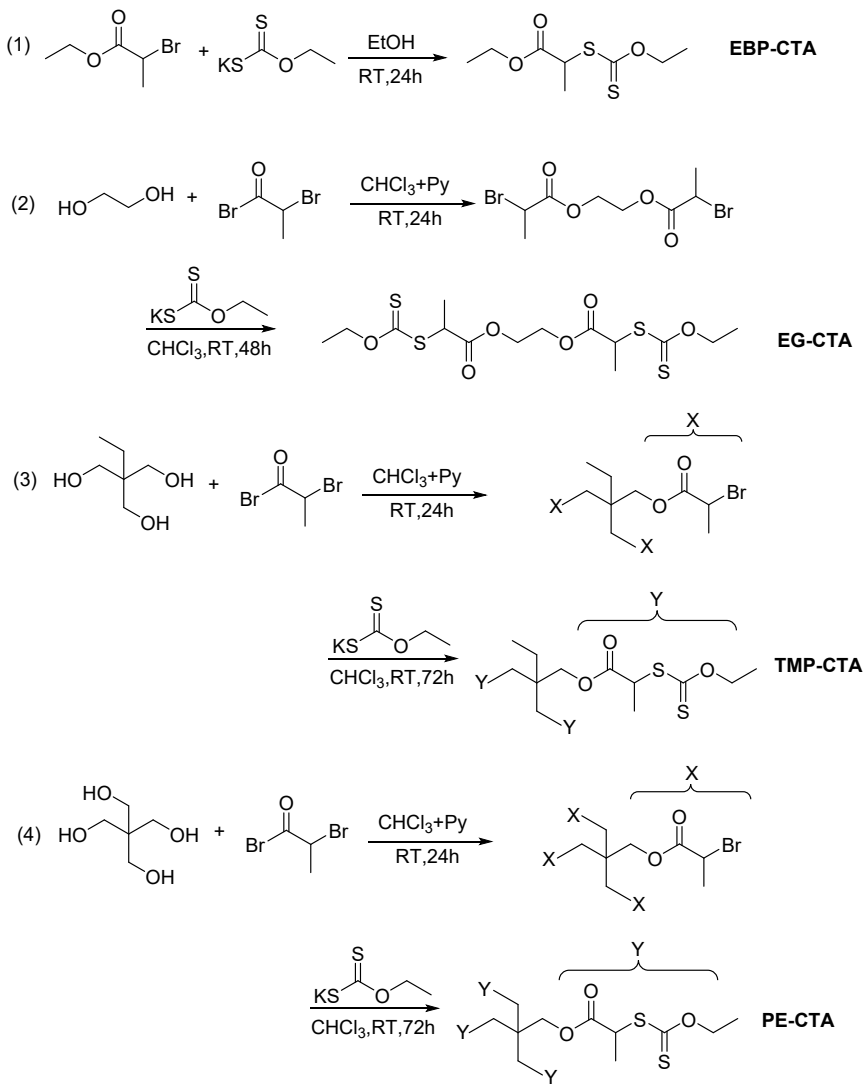

Scheme S1 Synthesis scheme of chain transfer agent.

Synthesis of monofunctional chain transfer agent EBP-CTA

EBP (5 g, 28 mmol), potassium ethyl xanthogenate (6.57 g, 41 mmol), anhydrous trichloromethane 220 mL were introduced to a 500 mL flask and kept magnetic stirring for 72 h at 60°C. The resultant white precipitate was filtered off. The filtrate was washed three times with 100 mL deionized water, dried over anhydrous magnesium sulfate and solvent was evaporated to dryness. The yellow colored liquid product was purified by column

chromatography using hexanes/ethyl acetate (30:1 v/v) as the eluent. 4.36 g EBP-CTA were received (yield: 70 %). The ^{1}H NMR spectrum was shown in Figure S1.

Synthesis of difunctional chain transfer agent EG-CTA

EG (2.0 g, 32.3 mmol) was dissolved in anhydrous pyridine (8 mL) and trichloromethane (48 mL). 2-Bromopropionyl bromide (17.4 g, 80.75 mmol) was added slowly to the ice-cooled solution. The ice bath was removed, and the mixture was stirred at ambient temperature for 48 h. Diluted hydrochloric acid (10%) was slowly added to the solution. The organic phase was then washed with 100 mL of aqueous $NaHCO_3$ (5 wt %) and finally dried with Mg_2SO_4. After evaporation of the solvent under reduced pressure, the product named EG-Br was purified by a double recrystallization in methanol (yield: 70 %). The molecular structure was verified by ^{1}H NMR spectrum (Figure S2).

The obtained EG-Br (4 g, 12.5 mmol), potassium ethyl xanthogenate (12.02g, 75 mmol), anhydrous trichloromethane 100 mL were introduced to a 250 mL flask and kept magnetic stirring for 72 h at 60°C. The resultant white precipitate was filtered off. The filtrate was washed three times with 100 mL deionized water, dried over anhydrous magnesium sulfate and solvent was evaporated to dryness. The yellow colored liquid product was purified by column chromatography using hexanes/ethyl acetate (20: 1 v/v) as the eluent. 3.85 g EG-CTA were received (yield: 70 %). The ^{1}H NMR spectrum was shown in Figure S3.

Synthesis of 3-armed chain transfer agent TMP-CTA

The 3-armed chain transfer agent TMP-CTA was synthesized from the trifunctional TMP agent following the same procedure above. The yellow colored liquid product was purified by column chromatography using hexanes/ethyl acetate (10: 1 v/v) as the eluent (yield: 71 %). The ^{1}H NMR spectrum was shown in Figure S4-S5.

Synthesis of 4-armed chain transfer agent PE-CTA

The 4-armed chain transfer agent PE-CTA was synthesized from the functional PE agent following the same procedure above. The yellow colored liquid product was purified by

column chromatography using hexanes/ethyl acetate (10: 1 v/v) as the eluent (yield: 60 %). The ^{1}H NMR spectrum was shown in Figure S6-S7.

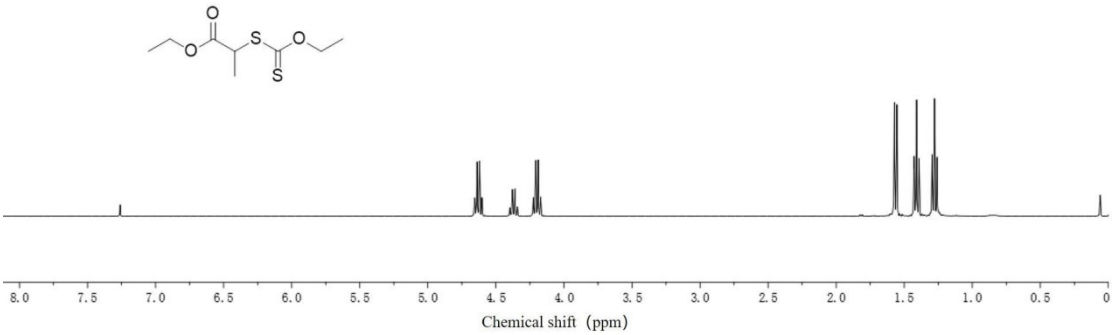

Figure S1 The ^{1}H NMR of EBP-CTA in $CDCl_3$.

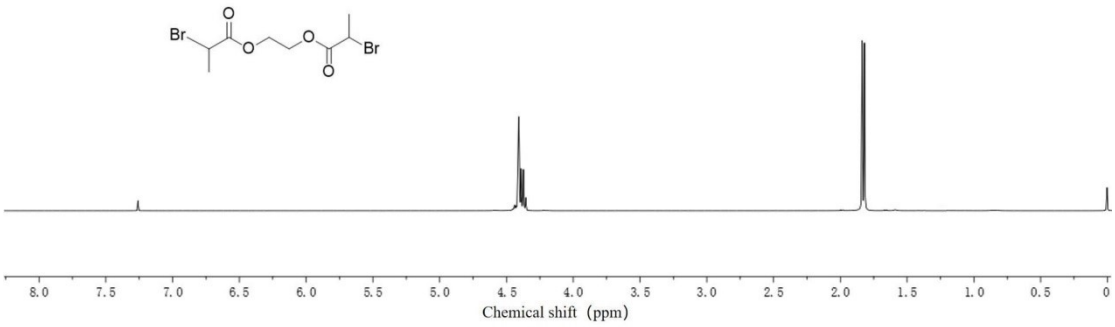

Figure S2 The ^{1}H NMR of EG-Br in $CDCl_3$.

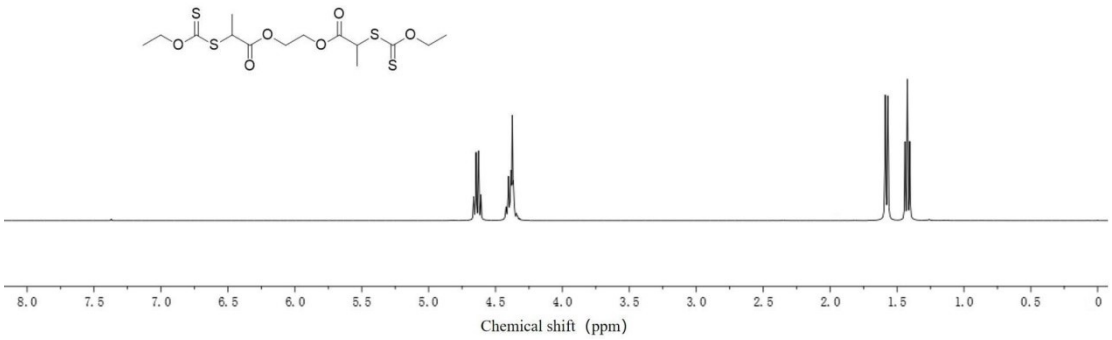

Figure S3 The ^{1}H NMR of EG-CTA in $CDCl_3$.

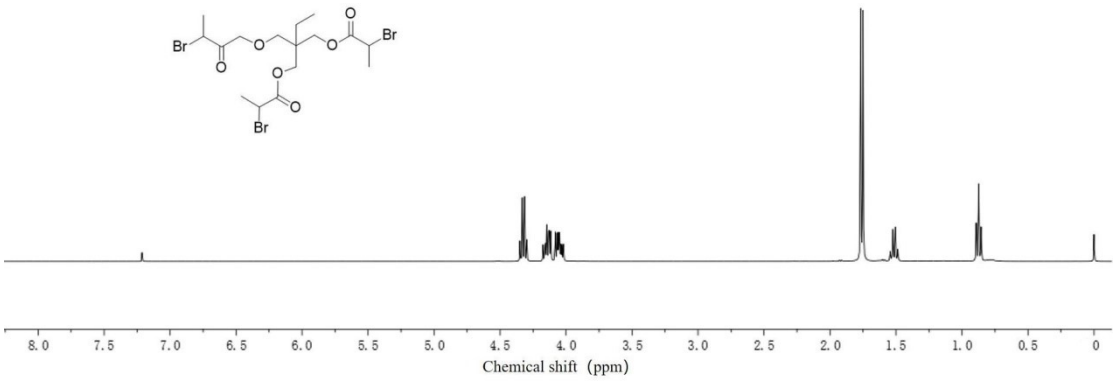

Figure S4 The ^{1}H NMR of TMP-Br in $CDCl_3$.

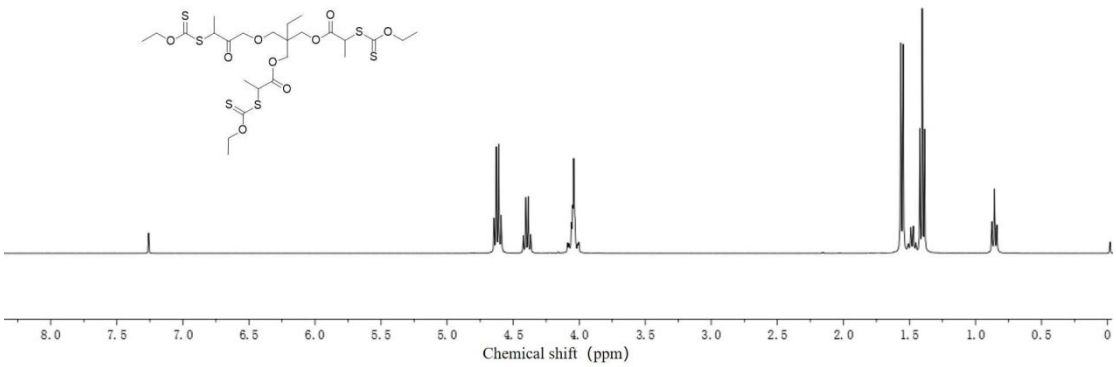

Figure S5 The ^{1}H NMR of TMP-CTA in $CDCl_3$.

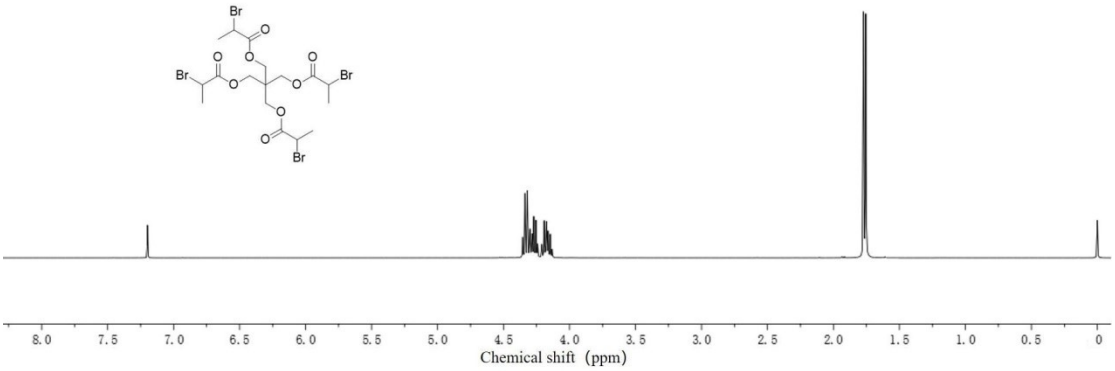

Figure S6 The ^{1}H NMR of PE-Br in $CDCl_3$.

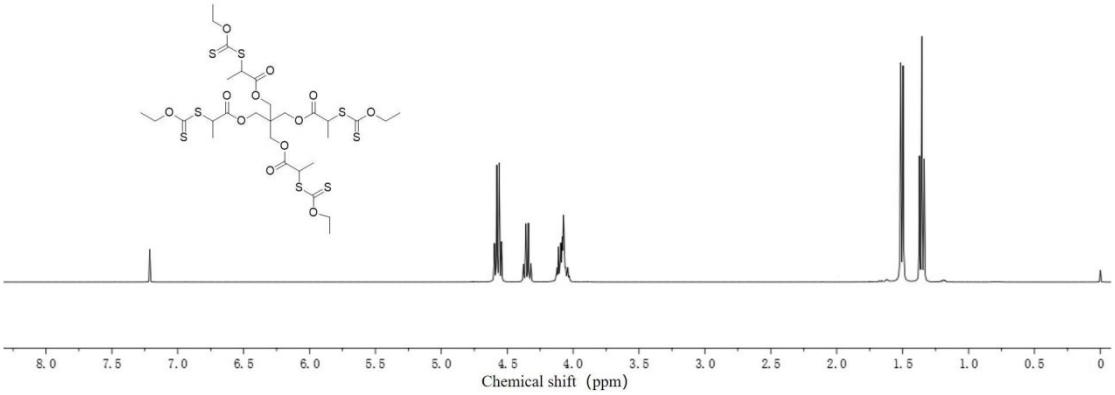

Figure S7 The ^{1}H NMR of PE-CTA in $CDCl_3$.

2. **Determination of the conversion by ^{1}H-NMR**

Conversion was determined by using the vinyl protons (δ=7.08 ppm, 1H) as a standard reference. Estimation of monomer/polymer ratio was calculated from the integration between δ=1.0-2.6 ppm, which correspond to the protons of both the NVP monomer (pyrrolidone backbone protons, 4 protons) and PVP polymer (6 protons per unit).

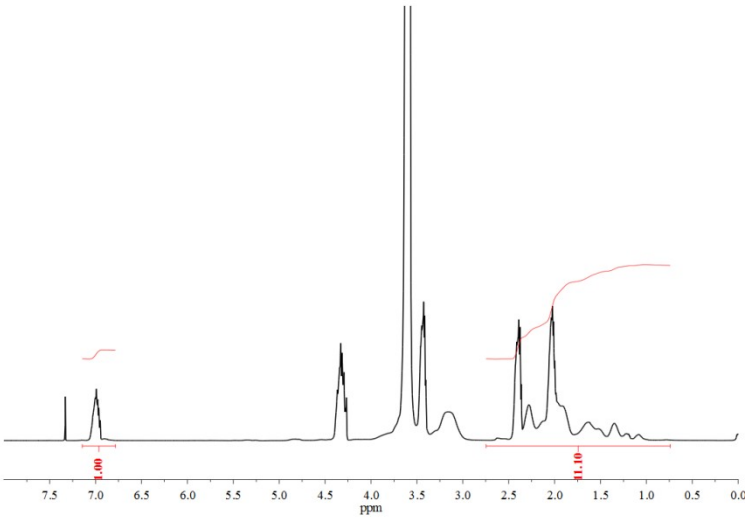

Figure S8 The ^{1}H NMR of the reaction mixture after 7.0 h of reaction time by using EBIB-CTA as the RAFT agent in $CDCl_3$.

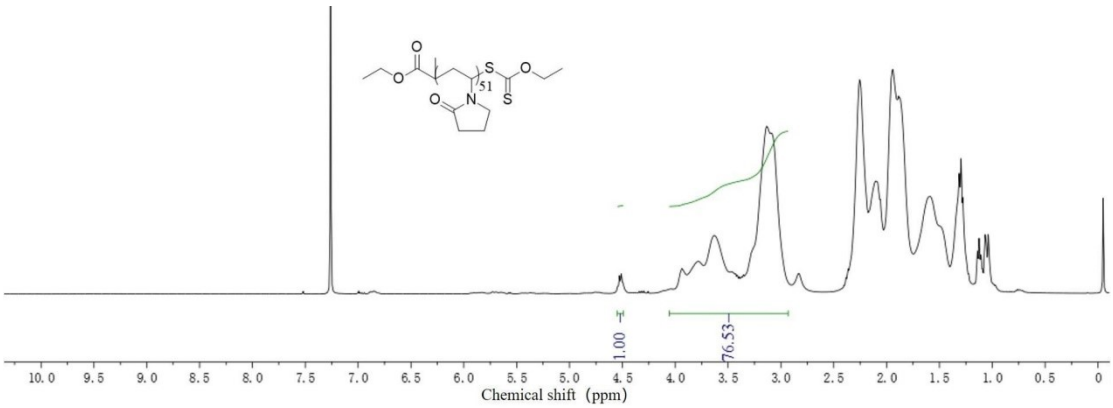

Figure S9 The ^{1}H NMR of PVP_{51}-CTA in $CDCl_3$.

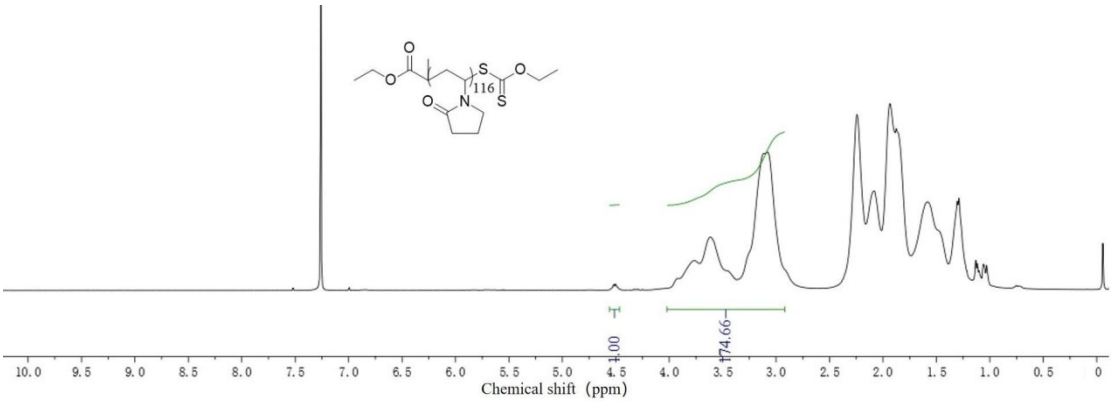

Figure S10 The ^{1}H NMR of PVP_{116}-CTA in $CDCl_3$.

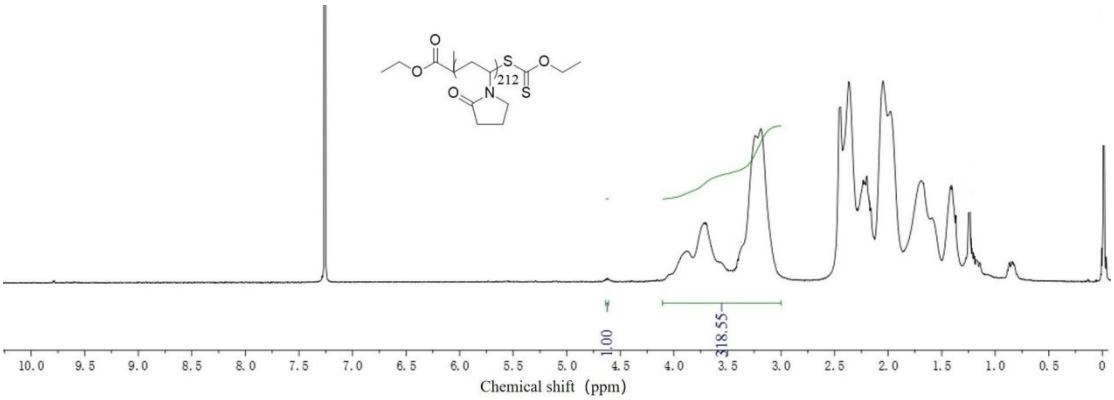

Figure S11 The ^{1}H NMR of PVP_{212}-CTA in $CDCl_3$.

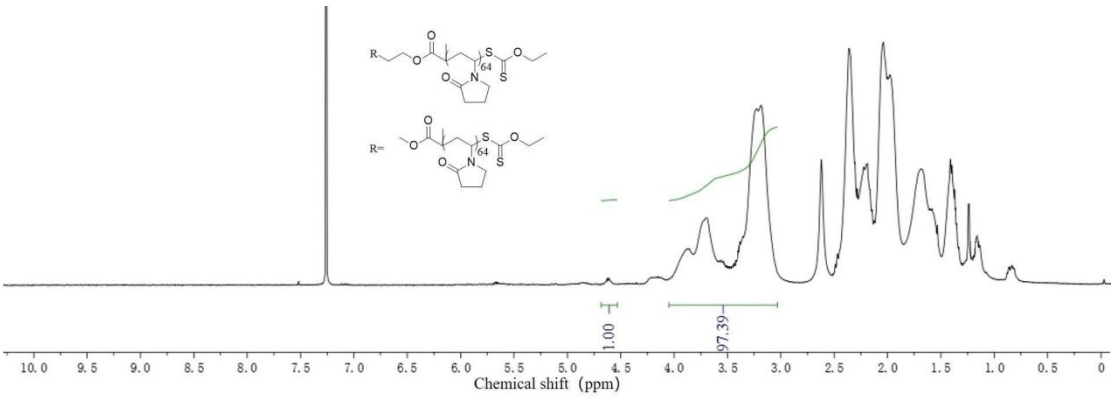

Figure S12 The ^{1}H NMR of CTA-PVP_{128}-CTA in $CDCl_3$.

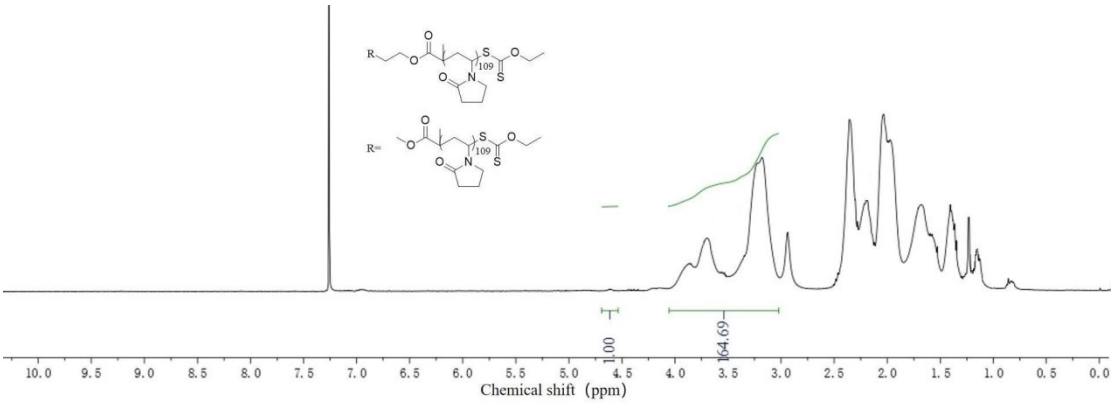

Figure S13 The ^{1}H NMR of CTA-PVP_{218}-CTA in $CDCl_3$.

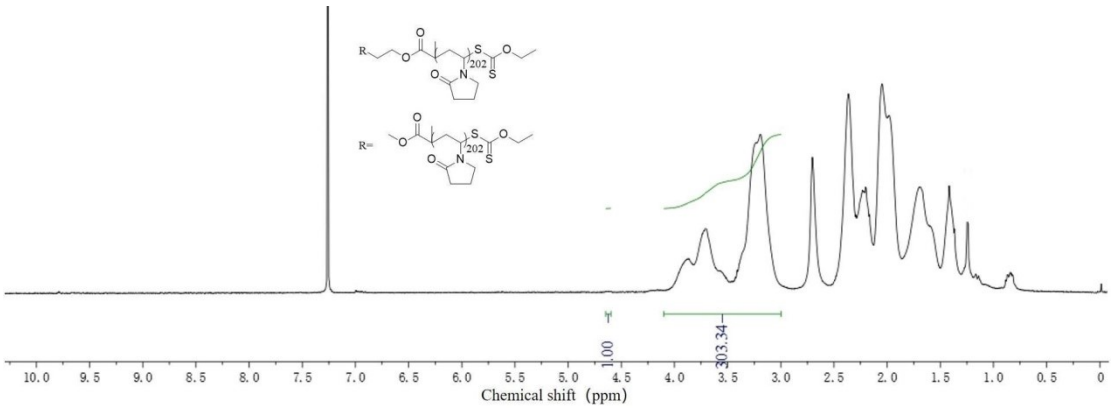

Figure S14 The ^{1}H NMR of CTA-PVP_{404}-CTA in $CDCl_3$.

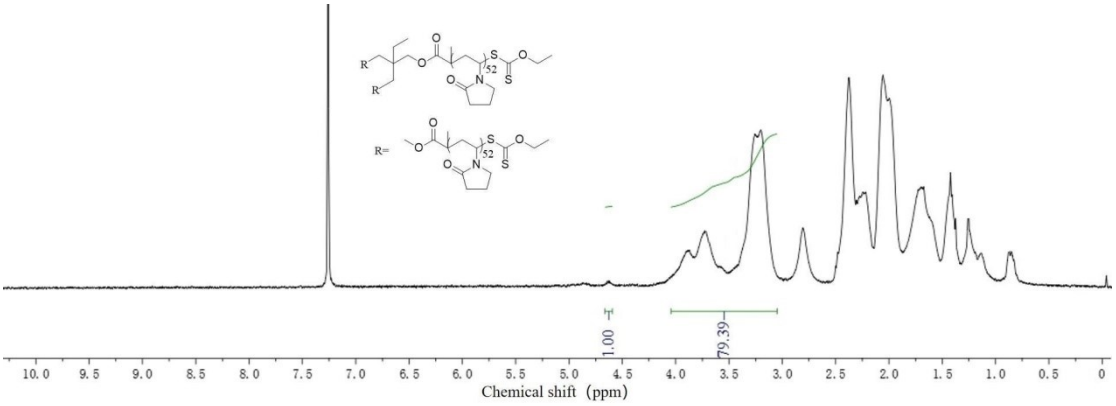

Figure S15 The ^{1}H NMR of 3S (PVP_{52}-CTA) in $CDCl_3$.

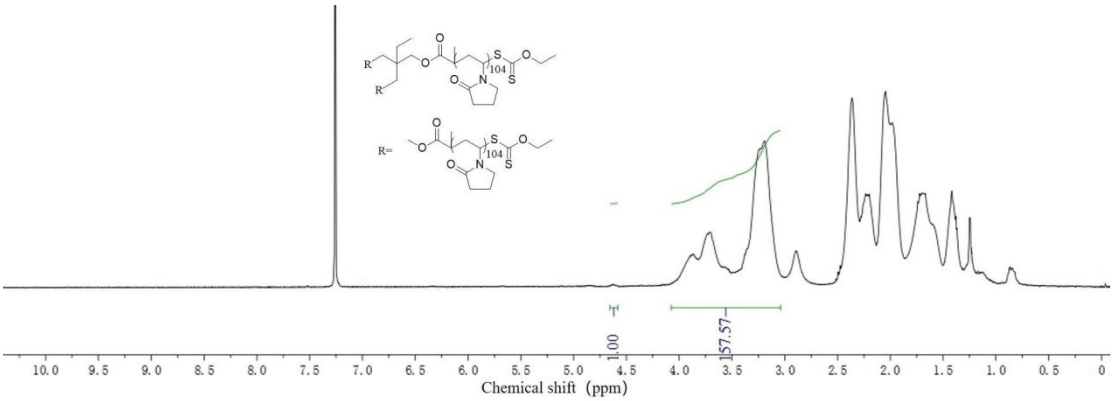

Figure S16 The ^{1}H NMR of 3S (PVP_{104}-CTA) in $CDCl_3$.

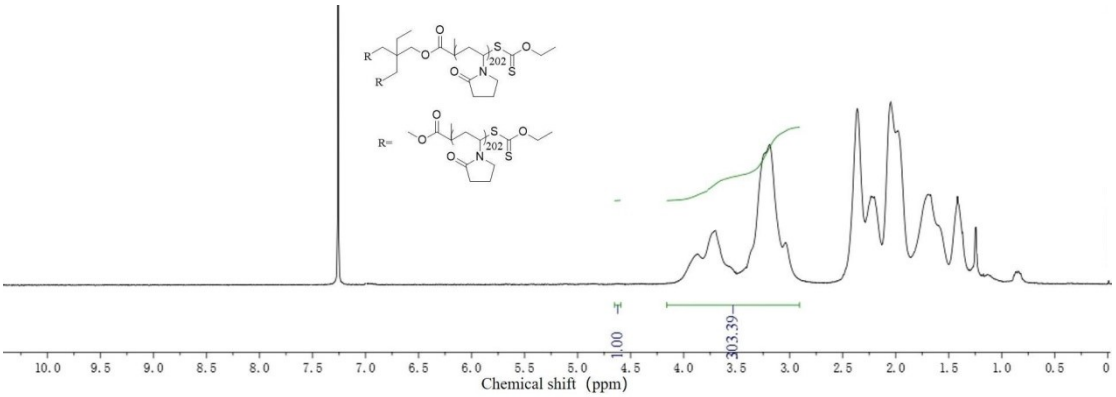

Figure S17 The ^{1}H NMR of 3S (PVP_{202}-CTA) in $CDCl_3$.

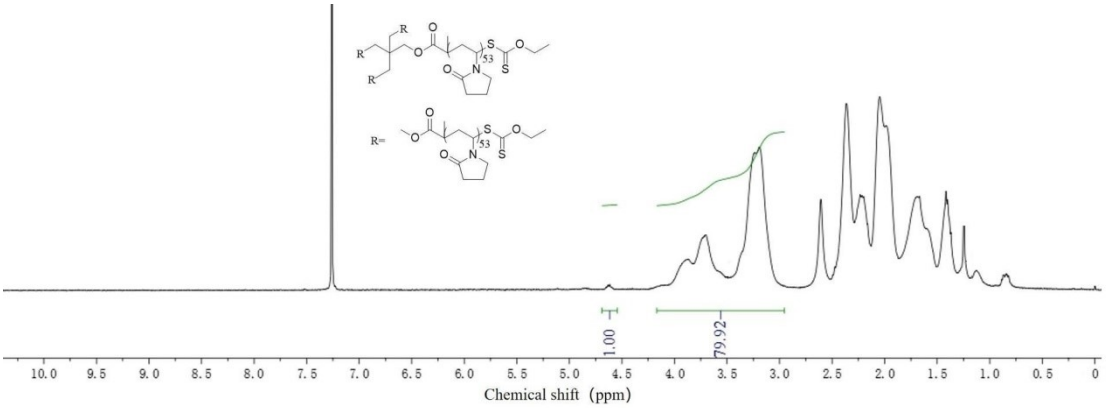

Figure S18 The ^{1}H NMR of 4S (PVP_{53}-CTA) in $CDCl_3$.

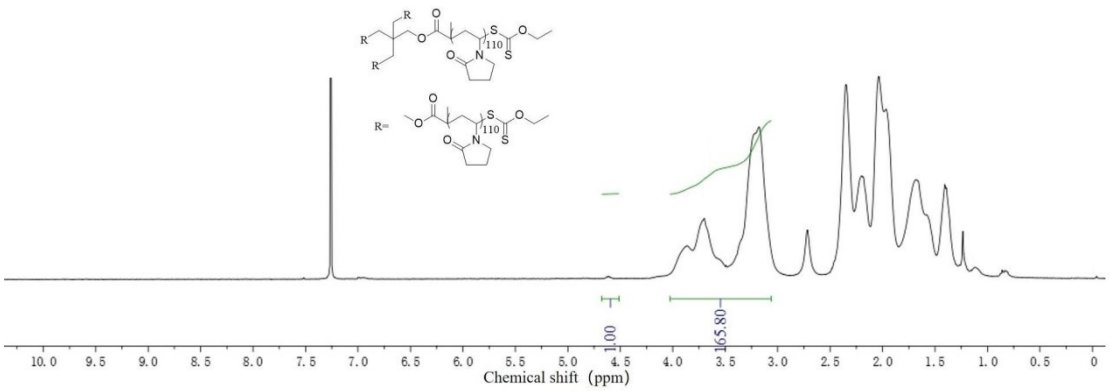

Figure S19 The ^{1}H NMR of 4S (PVP_{110}-CTA) in $CDCl_3$.

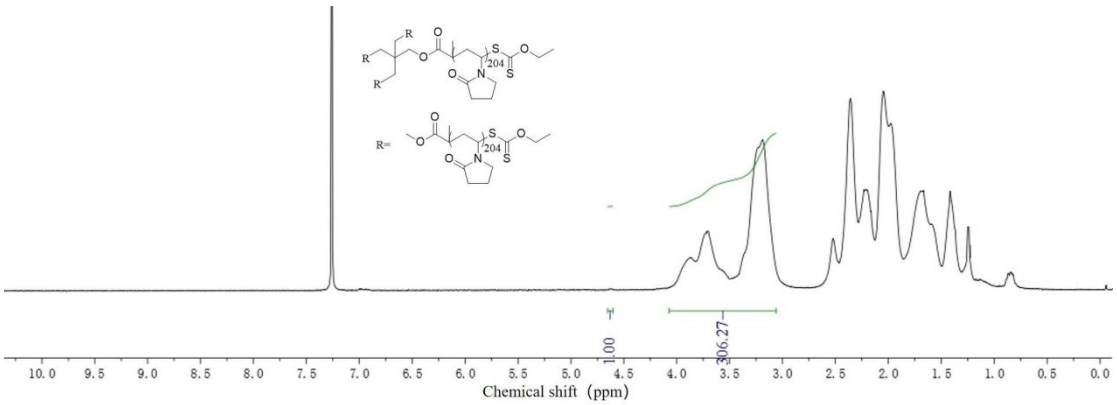

Figure S20 The ^{1}H NMR of 4S (PVP_{204}-CTA) in $CDCl_3$.

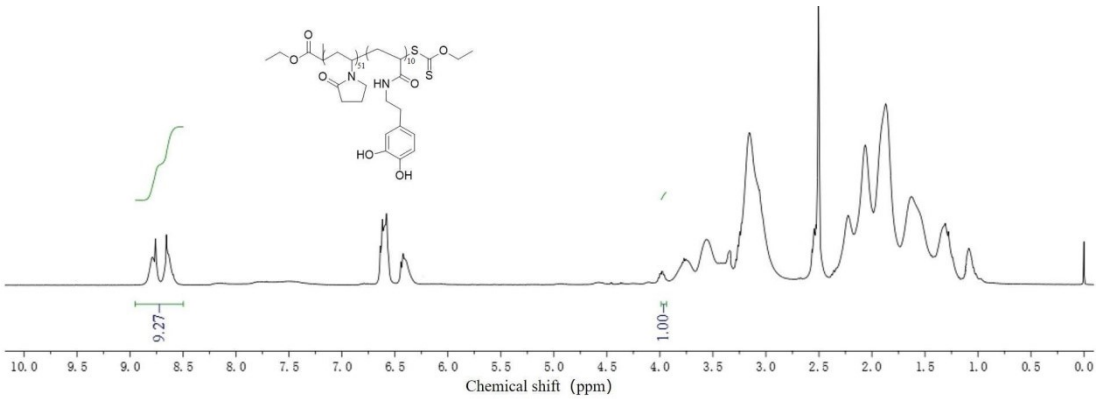

Figure S21 The ^{1}H NMR of PVP_{51}-$PDAA_{10}$ in DMSO-d_6.

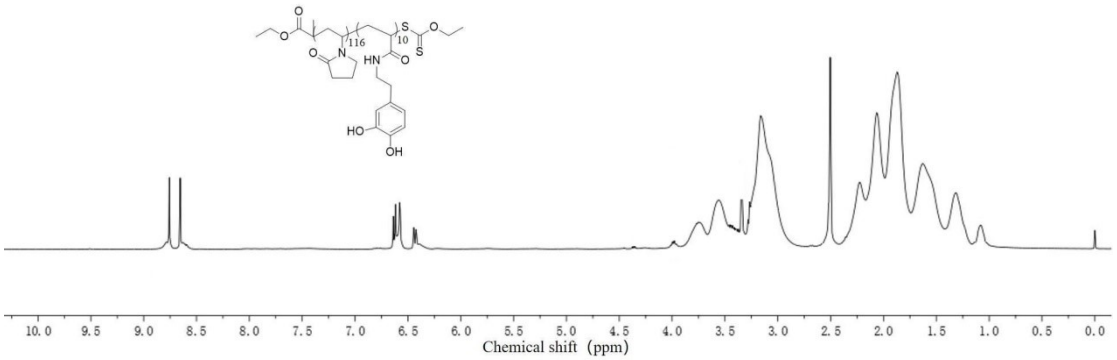

Figure S22 The ^{1}H NMR of PVP_{116}-$PDAA_{10}$ in DMSO-d_6.

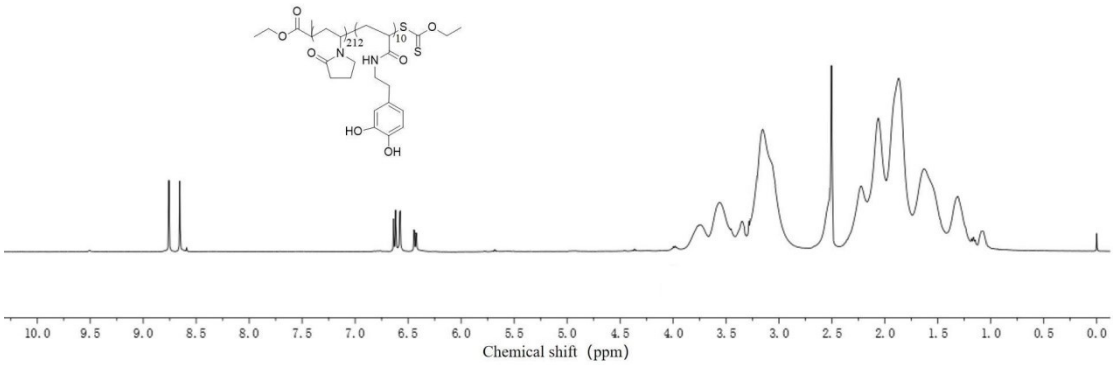

Figure S23 The ^{1}H NMR of PVP_{212}-$PDAA_{10}$ in DMSO-d_6.

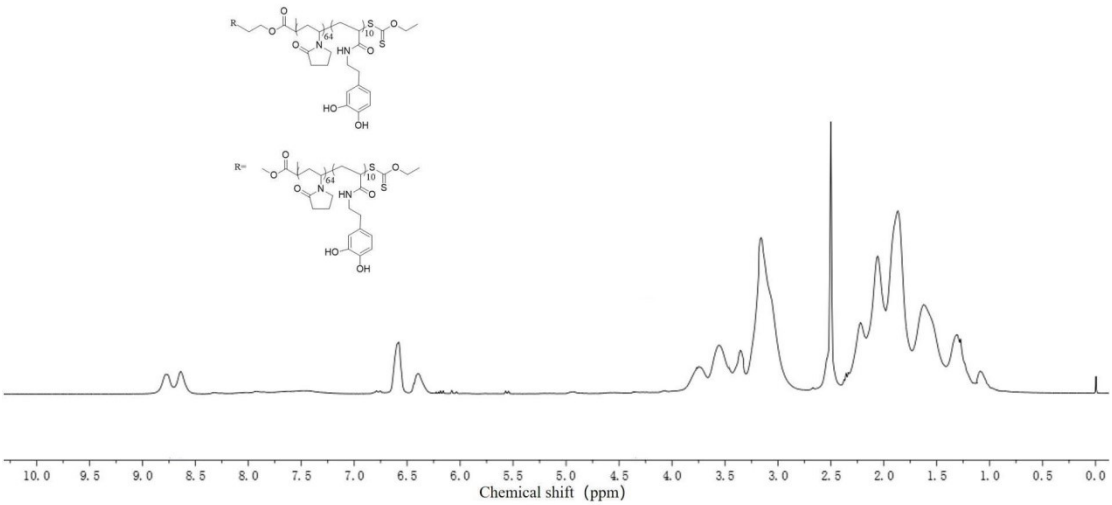

Figure S24 The ^{1}H NMR of $PDAA_{10}$-PVP_{128}-$PDAA_{10}$ in DMSO-d_6.

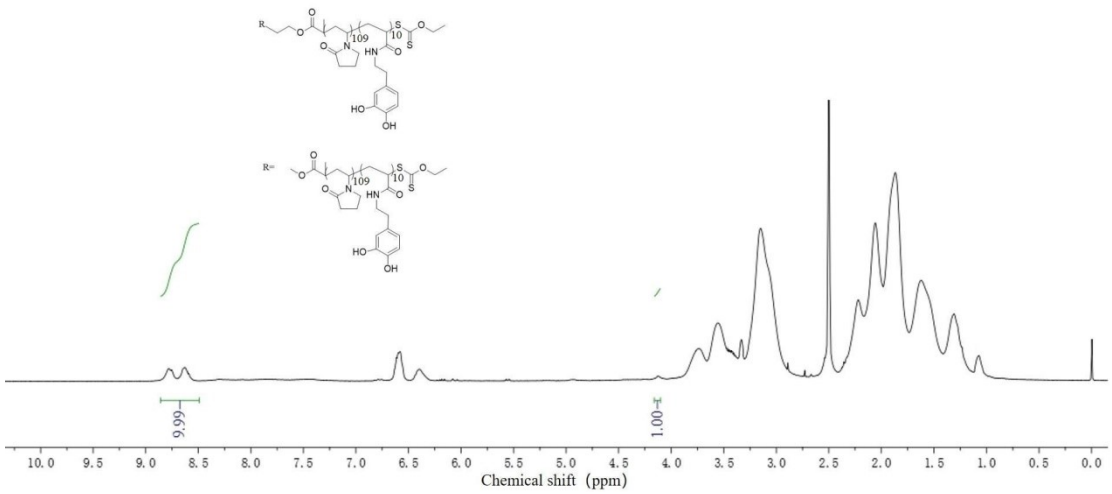

Figure S25 The ^{1}H NMR of $PDAA_{10}$-PVP_{218}-$PDAA_{10}$ in DMSO-d_6.

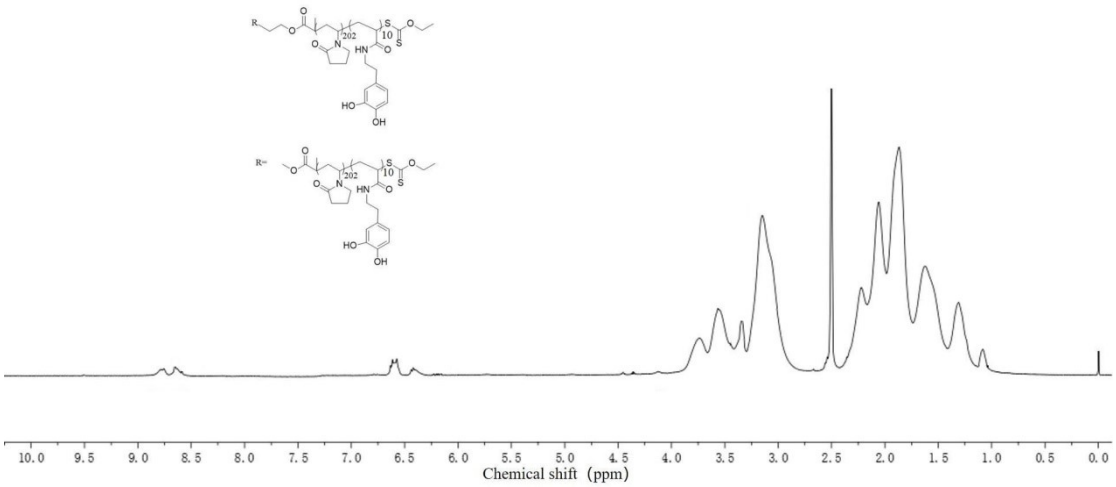

Figure S26 The ^{1}H NMR of $PDAA_{10}$-PVP_{404}-$PDAA_{10}$ in DMSO-d_6.

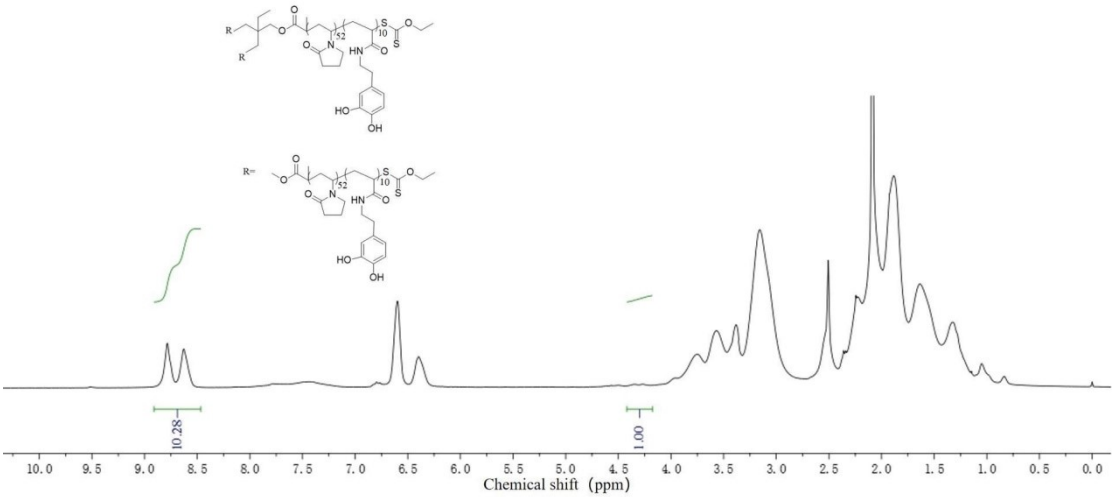

Figure S27 The ^{1}H NMR of 3-armed (PVP_{52}-$PDAA_{10}$) in DMSO-d_6.

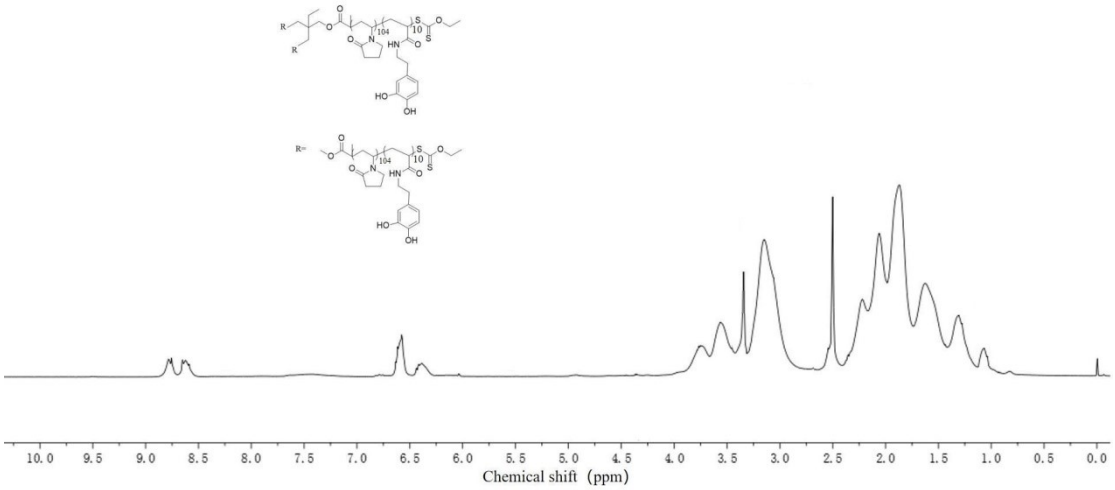

Figure S28 The ^{1}H NMR of 3-armed (PVP_{104}-$PDAA_{10}$) in DMSO-d_6.

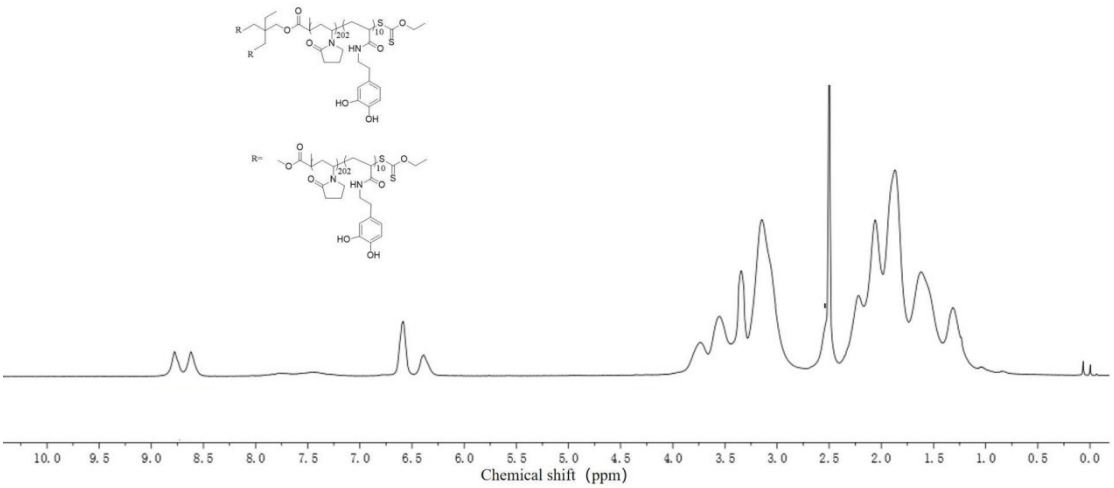

Figure S29 The ^{1}H NMR of 3-armed (PVP_{202}-$PDAA_{10}$) in DMSO-d_6.

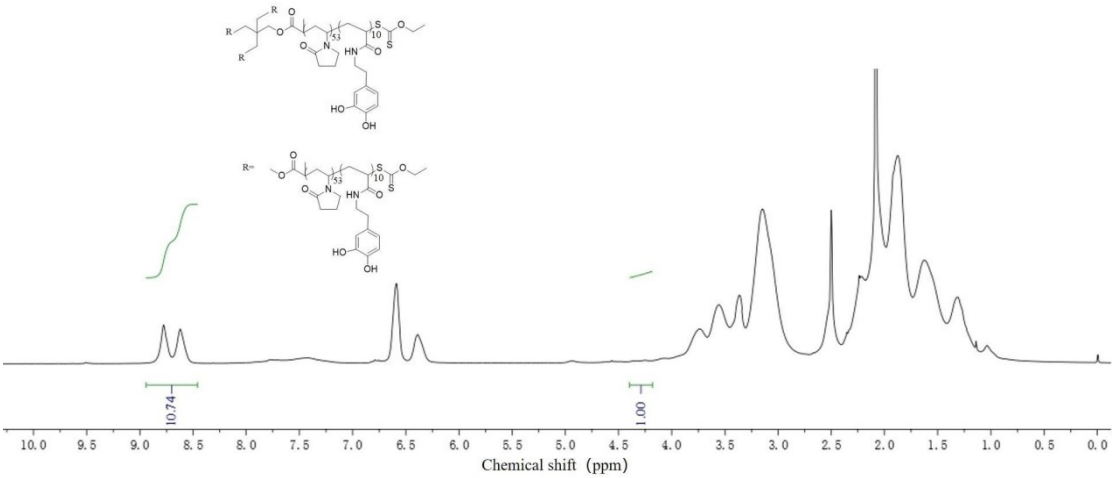

Figure S30 The ^{1}H NMR of 4-armed (PVP_{53}-$PDAA_{10}$) in DMSO-d_6.

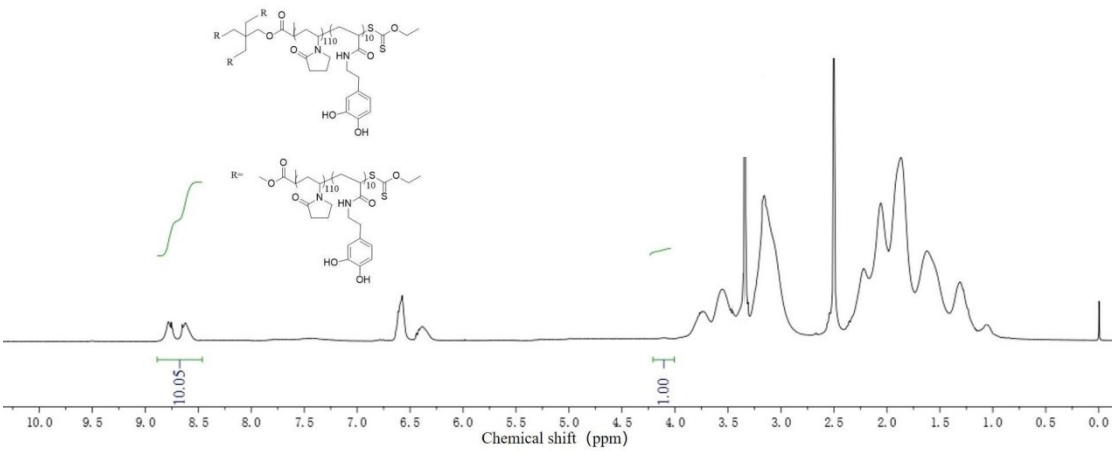

Figure S31 The ^{1}H NMR of 4-armed (PVP_{110}-$PDAA_{10}$) in DMSO-d_6.

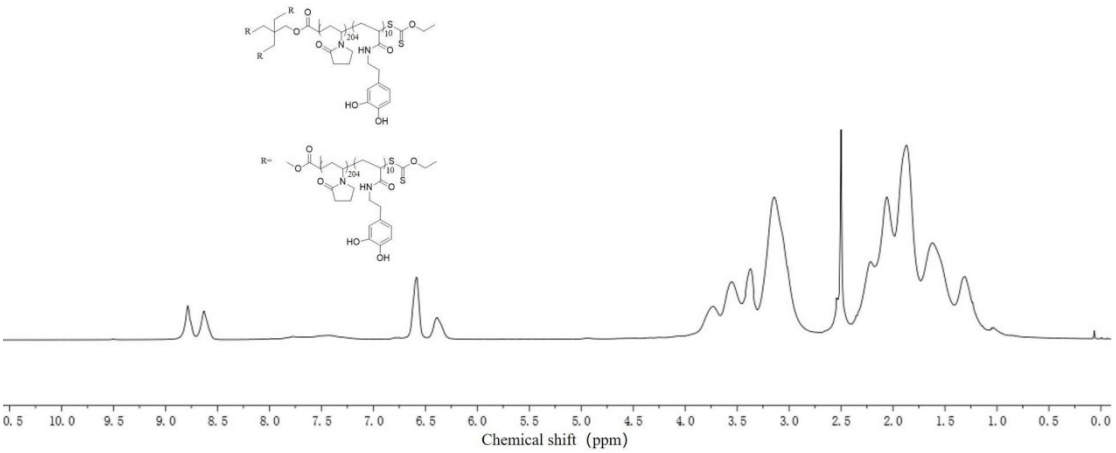

Figure S32 The ^{1}H NMR of 4-armed (PVP_{204}-$PDAA_{10}$) in DMSO-d_6.

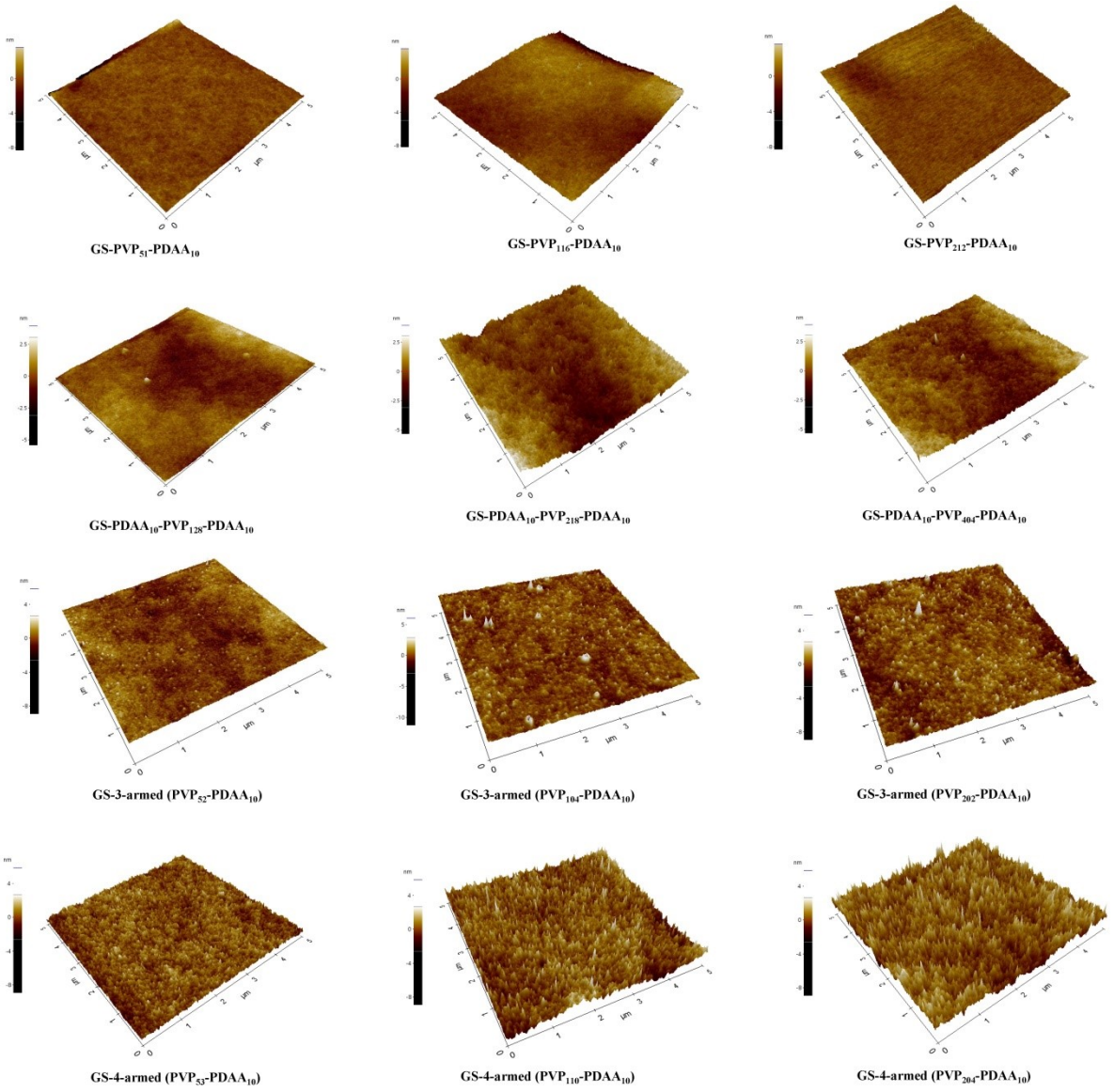

Figure S33 AFM images of block copolymer-anchored GS surfaces.

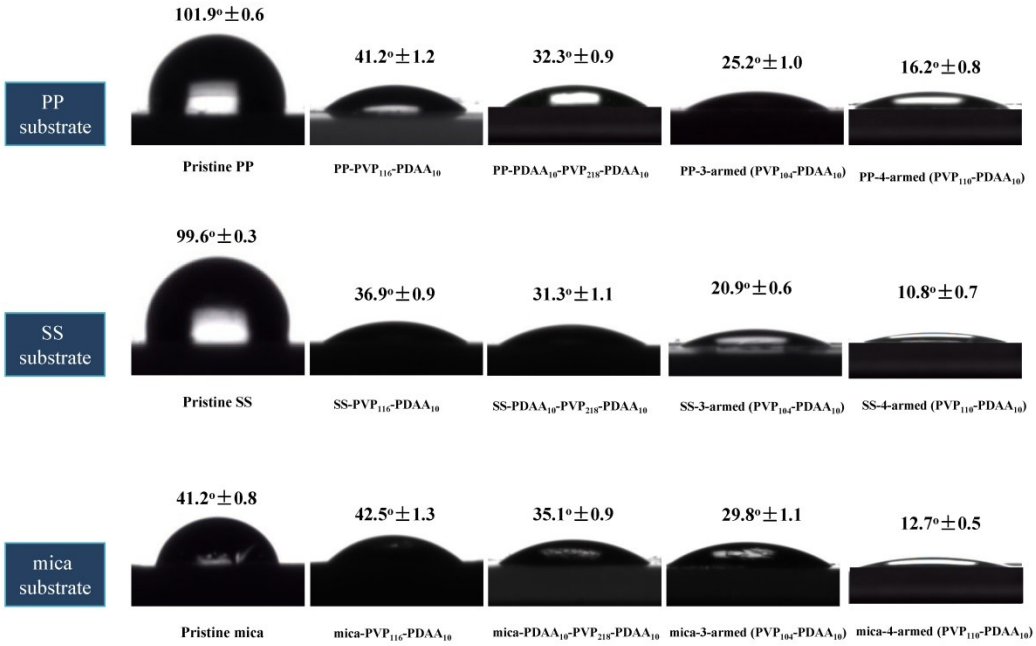

Figure S34 Water contact angle of pristine PP, SS, mica, PP-PVP_{116}-$PDAA_{10}$, PP-$PDAA_{10}$-PVP_{218}-$PDAA_{10}$, PP-3-armed (PVP_{104}-$PDAA_{10}$), PP-4-armed (PVP_{110}-$PDAA_{10}$), SS-PVP_{116}-$PDAA_{10}$, SS-$PDAA_{10}$-PVP_{218}-$PDAA_{10}$, SS-3-armed (PVP_{104}-$PDAA_{10}$), SS-4-armed (PVP_{110}-$PDAA_{10}$), mica-PVP_{116}-$PDAA_{10}$, mica-$PDAA_{10}$-PVP_{218}-$PDAA_{10}$, mica-3-armed (PVP_{104}-$PDAA_{10}$), mica-4-armed (PVP_{110}-$PDAA_{10}$) and the photomicrographs of the droplet attached on the pristine and modified surfaces. The values over the droplet represent the average value of the water contact angle.

Figure S35 Scouring test of coating under the faucet (glass substrate).

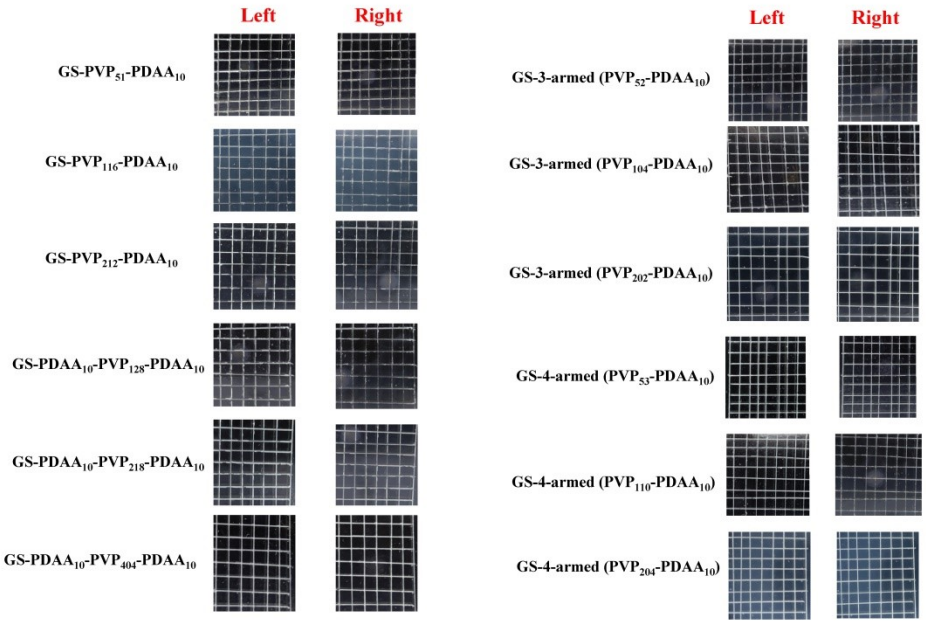

Figure S36 The photo images of before (left) and after (right) the adhesion test based on the cross-cut method.

In order to quantitative evaluate the adhesion, thicker coatings (~1 μm) were prepared and a cross-cut method was employed to evaluate the grade of adhesion of the formed coatings. The cross-cut method is a generally procedure to qualitatively evaluate the adhesion of polymeric coating upon substrate and the adhesion is demarcated from 1B to 5B according to the ASTM D3359 scale. The higher the value, the better the adhesion. The level 5B indicates no detachment of square lattices from the substrate surface and the edges are completely smooth. In our case, the adhesion of coatings was at the highest level (5B) on both substrates.

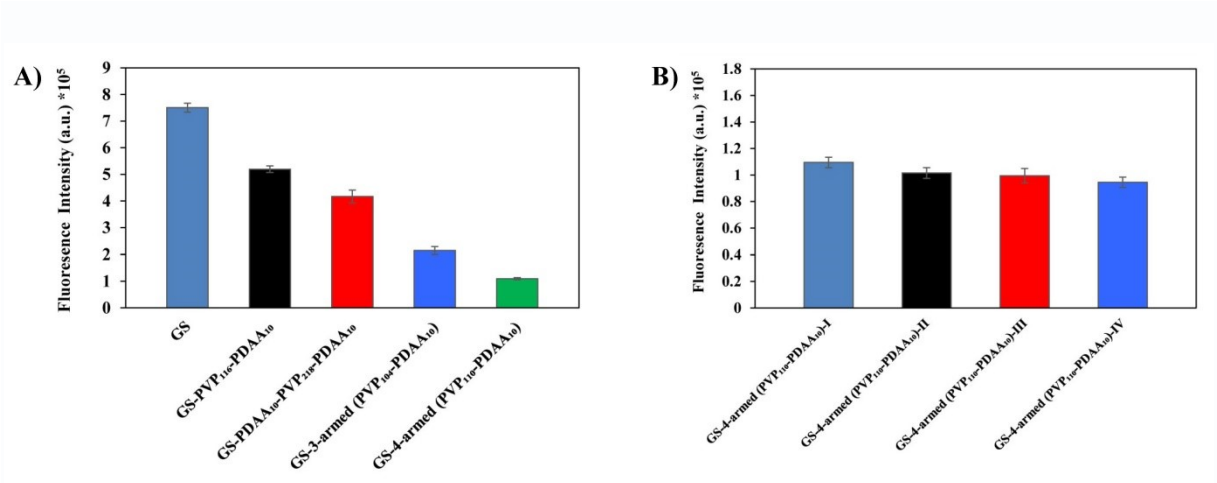

Figure S37 A) Fluorescence intensities of the coatings with similar thickness and different topology after exposure to BSA-FITC solution, B) fluorescence intensities of the coatings with same topology and different thickness after exposure to BSA-FITC solution. The substrate is glass and the average thickness of block copolymer-anchored GS surfaces was shown in Table S3.

Table S1 Characterization of PVP macro-chain transfer agents

Run	Composition[a]	M_n (KDa)		Đ[d]
		GPC[b]	NMR[c]	
1	PVP_{51}-CTA	10	5.9	1.08
2	PVP_{116}-CTA	15	13	1.08
3	PVP_{212}-CTA	31	24	1.10
4	CTA-PVP_{128}-CTA	20	15	1.12
5	CTA-PVP_{218}-CTA	38	25	1.11
6	CTA-PVP_{404}-CTA	54	45	1.12
7	3-armed (PVP_{52}-CTA)	22	18	1.13
8	3-armed (PVP_{104}-CTA)	53	36	1.11
9	3-armed (PVP_{202}-CTA)	91	68	1.12
10	4-armed (PVP_{53}-CTA)	26	25	1.09
11	4-armed (PVP_{110}-CTA)	59	50	1.12
12	4-armed (PVP_{204}-CTA)	97	92	1.11

[a] The subscript numbers represent the repeating units number of each block determined by ^{1}H NMR.

[b] M_n determined by GPC using poly(methyl methacrylate) standards for calibration.

[c] M_n calculated from ^{1}H NMR measurements.

[d] Đ represent the molecular weight distribution index.

Table S2 The average roughness and thickness of block copolymer-anchored GS surfaces.

	Average roughness[a]/nm	Thickness/nm	Average mass of the copolymers forming the coating/ng·cm^{-2}
GS-PVP_{51}-$PDAA_{10}$	0.75	2.54±0.26	670
GS-PVP_{116}-$PDAA_{10}$	0.68	3.52±0.31	851
Gs-PVP_{212}-$PDAA_{10}$	0.79	4.52±0.36	1030
GS-$PDAA_{10}$-PVP_{128}-$PDAA_{10}$	0.62	4.65±0.55	721
GS-$PDAA_{10}$-PVP_{218}-$PDAA_{10}$	0.85	6.85±0.62	810
GS-$PDAA_{10}$-PVP_{404}-$PDAA_{10}$	0.89	8.54±0.41	990
GS-3-armed (PVP_{52}-$PDAA_{10}$)	1.76	9.68±0.82	912
GS-3-armed (PVP_{104}-$PDAA_{10}$)	1.88	11.25±0.76	1070
GS-3-armed (PVP_{202}-$PDAA_{10}$)	2.02	14.62±0.64	1280
GS-4-armed (PVP_{53}-$PDAA_{10}$)	3.32	14.86±0.66	952
GS-4-armed (PVP_{110}-$PDAA_{10}$)	3.68	17.85±0.87	1138
GS-4-armed (PVP_{204}-$PDAA_{10}$)	3.78	21.25±0.75	1350

[a] the value was obtained from AFM.

Table S3 The average thickness of block copolymer-anchored GS surfaces.

	Thickness/nm
GS-PVP_{116}-$PDAA_{10}$	18.32±0.51
GS-$PDAA_{10}$-PVP_{218}-$PDAA_{10}$	17.28±0.62
GS-3-armed (PVP_{104}-$PDAA_{10}$)	19.15±0.76
GS-4-armed (PVP_{110}-$PDAA_{10}$)	17.85±0.87
GS-4-armed (PVP_{110}-$PDAA_{10}$)-I	17.85±0.87
GS-4-armed (PVP_{110}-$PDAA_{10}$)-II	28.56±0.62
GS-4-armed (PVP_{110}-$PDAA_{10}$)-III	49.37±0.76
GS-4-armed (PVP_{110}-$PDAA_{10}$)-IV	76.62±0.51